ISBN: 978-3-95450-247-9 ISSN: 2673-5490 doi: 10.18429/JACoW-IPAC2024-WEPG72

FAST LASER FOCAL POSITION CORRECTION USING DEPLOYED MODELS

N. Cook*, S. Coleman, J. Einstein-Curtis
RadiaSoft, Boulder, Colorado, USA
S. Barber, C. Berger, K. Jensen, J. van Tilborg
Lawrence Berkeley National Laboratory, Berkeley, CA, USA

Abstract

Ultrafast high repetition-rate laser systems are essential to modern scientific and industrial applications. Variations in critical figures of merit, such as focal position, can significantly impact efficacy for applications involving laser plasma interactions, such as electron beam acceleration and radiation generation. We present a diagnostic and correction scheme for controlling and determining laser focal position by utilizing fast wavefront sensor measurements from multiple positions to train a focal position predictor. We present the deployment and testing of this scheme at the BELLA Center at Lawrence Berkeley National Laboratory. Online optical adjustments are made to a telescopic lens to provide the desired correction on millisecond timescales. A framework for generating a low-level hardware description of ML-based correction algorithms on FPGA hardware is coupled directly to the beamline using the AMD Xilinx Vitis AI toolchain in conjunction with deployment scripts.

INTRODUCTION

Laser plasma accelerators (LPAs) rely upon accurate control of ultrafast lasers, typically Ti:Sapph and Nd:Yag amplifier systems [1]. The BELLA Center at Lawerence Berkeley National Laboratory (LBNL) features several ultra-short pulse, high-energy beamlines to develop LPAs. These accelerators require highly repeatable, stable interaction points to generate high-quality electron beams, which necessitates a collection of active and passive controls to mitigate environmental, mechanical, and component variations.

Recent work has primarily focused on enhancing transverse beam stability [2]. This paper describes a a strategy to address focal position stability, leveraging a machine learning (ML) enhanced wavefront diagnostic in tandem with a Field Programmable Gate Array (FPGA) controller to correct focal position at a kHz-scale rate. By building a model of wavefront at the interaction point, it is possible to use a non-perturbative measurement to calculate the focal position. Here we report on progress in implementing such a control scheme using a simple fast diagnostic and control scheme.

FACILITY AND EQUIPMENT

The focal position control system was developed for use with the HTU laser system at the BELLA Center. Figure 1 depicts a schematic of the beamline with the controller elements highlighted. The beamline operates with 1 kHz seed pulses and a 1 Hz full-power pulse. A Thorlabs WFS20-7AR is used to parasitically capture light from the 1 kHz seed pulses, as indicated by "Near-field Camera 3" in the diagram. A HASO FIRST Shack-Hartmann wavefront sensor was used as the ground-truth imaging device for assessing performance of the WFS20, as indicated by "Far-field" camera in the diagram. We employ a Zaber Motion X-LDA-A linear stage to move a transmissive lens in the beam expander section of the laser; previous analyses were performed to determine the best location for the lens and to correlate the focal position change as a function of lens position.

Acquisition settings are controlled via a custom Python library, which leverages the Thorlabs WFS20 driver API to manage acquisition, processing, and control of the camera. The same library employs a custom API for the Zaber stage, using the device's native ASCII protocol to enable asynchronous control during operations. The maximum acceleration and velocity of the stage were limited by using a manufacturer-provided toolkit. Additional features, such as motion averaging and control loop tolerance, can also be controlled through the application. For the test data shown below, the stage was operated in a mode that permits faster response times at the cost of reduced precision by streaming updated positions to the controller as opposed to waiting for moves to complete.

A Xilinx Zynq ZCU104 FPGA evaluation kit was used for testing to provide flexibility during the prototype phase, including a variety of customizable I/O, well-supported manufacturer-provided software, and a variety of processing options in support of ML operations. Initial tests indicate support for kHz-scale processing of input signals [3]. Although this device was deployed at the beamline, the data collected and shown below does not employ an ML algorithm via the FPGA platform.

RESULTS & DISCUSSION

With this controller in place, we performed a series of tests under different operating conditions. For these initial tests, a PID control algorithm is employed; the PID was tuned using the Ziegler–Nichols method based on initial data acquisition. The first set of tests was performed at low power, evaluating the performance of the 1 kHz seed pulse with the longitudinal focal control system (LFS) on and off. For all data, wavefronts were taken with 1 ms exposure time and default stage settings. A polynomial fitting is performed in the camera and Thorlabs driver, and the Zernike coefficients corresponding to radius of curvature are returned to the controller after each capture. Figure 2 depicts the measured radius of curvature over time for a 15 minute sample.

A histogram of the measured radius of curvature values is shown in Fig. 3, indicating the range of deviations from the

* ncook@radiasoft.net

ISBN: 978-3-95450-247-9 ISSN: 2673-5490 doi: 10.18429/JACoW-IPAC2024-WEPG72

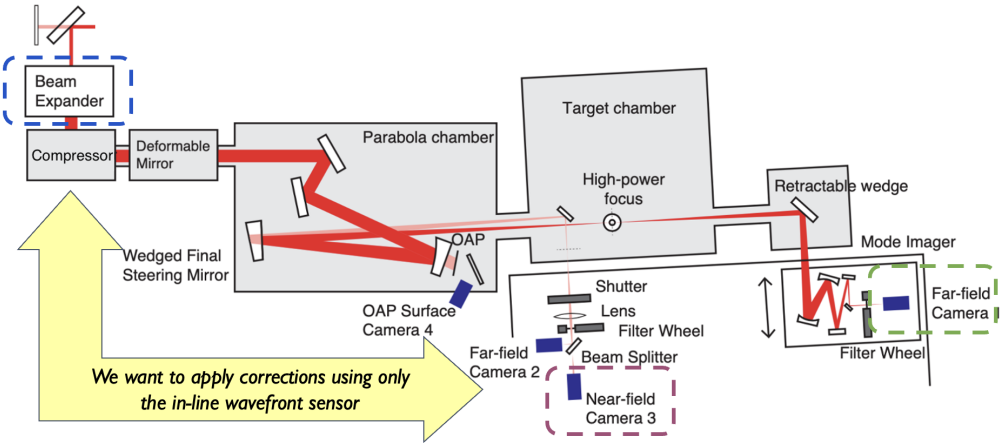

Figure 1: Diagram of HTU laser system at LBNL, highlighting the proposed correction scheme. Machine learning techniques are used to correlate a fast, non-perturbative sensor with a high-quality, but perturbative wavefront sensor which cannot be used for online correction. The resulting online diagnostic is used to deduce variations away from the desired focal position, which is then corrected for prior to the next shot by changes made to a transmissive lens beam expander.

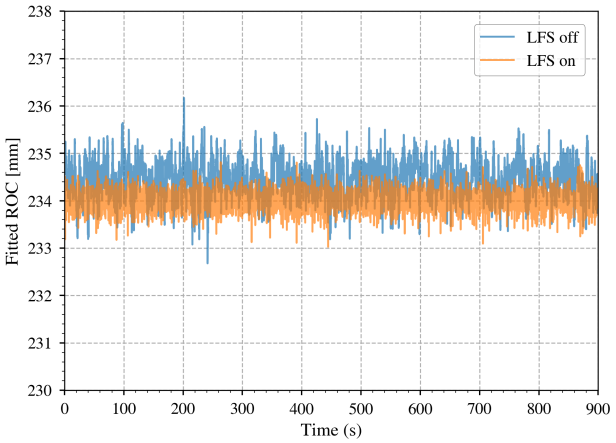

Figure 2: A sample of radius of curvature measurements taken during low power operation, with and without the focal position corrector in use.

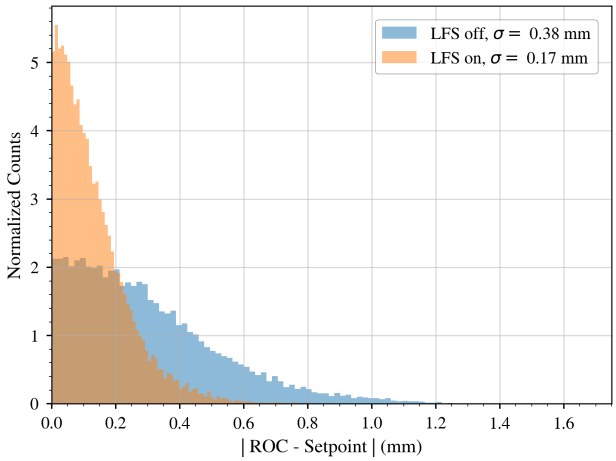

Figure 3: Distribution of focal position deviations as determined from radius of curvature (ROC) estimates during low power operation, with and without the focal position corrector in use. The corrector reduced standard deviation in ROC from 0.38 mm to 0.17 mm.

setpoint. Without the LFS active, the standard deviation in the radius of curvature is 0.38 mm; use of the LFS improves this to 0.17mm. Maximum excursions are similarly reduced from ~ 1.2 mm down to ~ 0.6 mm. Figure 4 presents the normalized frequency content of the signal up to 5 Hz. We note that signals below 1 Hz are greatly diminished, indicating that slow variations in the radius of curvature are being corrected for by the LFS. Corresponding higher frequency content does increase, indicating some contribution of stage motion. Additional datasets were then taken for high power operation, during which fully amplified pulses were produced at a 1 Hz rate. A shutter is engaged to prevent damage to the seed pulse WFS during the high power interval every second. Radius of curvature data is still extracted for the low power seed pulse at all other times. Figure 5 depicts the focal position deviations during high power operation. As with the low power signal, the LFS reduces the standard deviation in the radius of curvature by greater than a factor of 2, from 0.42 mm down to 0.22 mm. Again, maximum excursions are similarly reduced, this time from ~ 1.6 mm down to ~ 0.8 mm. Figure 6 presents the normalized frequency content of the signal up to 5 Hz for these tests. As with low power operation, we note that signals below 1 Hz are greatly diminished, indicating that slow variations in the radius of curvature are being corrected for by the LFS, but that some higher frequency content is introduced. However, the use of a fast shutter to protect the diagnostics introduces peaks in the frequency analysis at 1 Hz and its harmonics. These have been filtered out from the included figure. Work is ongoing to evaluate the frequency content and characterize other sources of jitter in the system during high power performance.

ISBN: 978-3-95450-247-9 ISSN: 2673-5490 doi: 10.18429/JACoW-IPAC2024-WEPG72

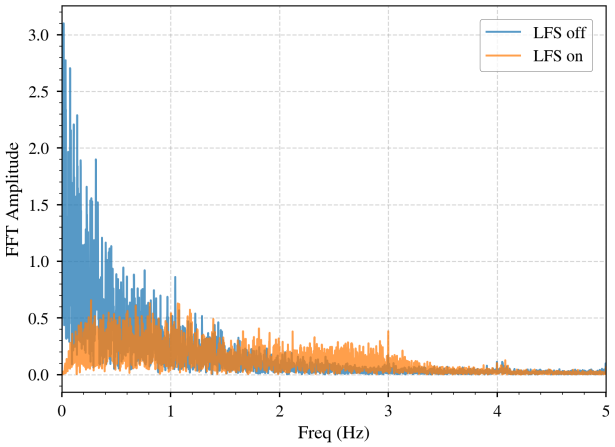

Figure 4: Normalized frequency spectrum of measured ROC during low power operation, with and without the focal position corrector in use. It can be seen that slow variations, below 1-2 Hz, are significantly reduced.

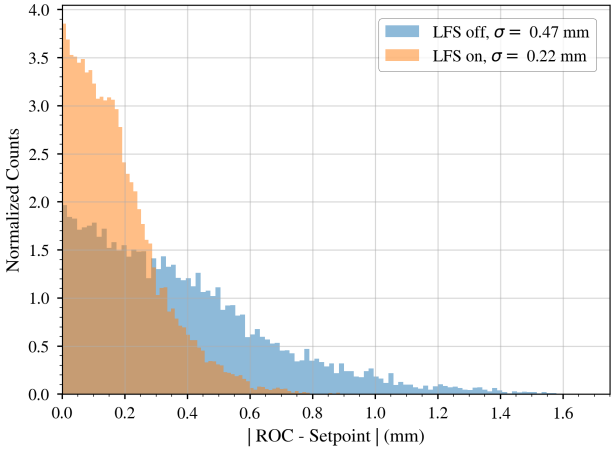

Figure 5: Distribution of focal position deviations as determined from radius of curvature (ROC) estimates during high power operation, with and without the focal position corrector in use. The corrector reduced standard deviation in ROC from 0.47 mm to 0.22 mm.

CONCLUSION

We have demonstrated the development and use of a focal position correction system operating at the BELLA Center HTU beamline. Our strategy is to leverage an upstream wavefront sensor to inform a fast moving stage. The corrector integrates an asynchronous controller to coordinate wavefront capture and subsequent stage motion at a few Hz. Using this system, variations in the focal position are reduced by greater than a factor of two, during both low and high power operations. Maximum excursions are similarly reduced. Work is ongoing to evaluate any corrector influence on electron beam quality from the resulting laser plasma interaction. Future work will explore the integration of machine learning techniques to improve diagnostic fidelity and to inform better stage position updates, enabling higher quality and higher bandwidth corrections.

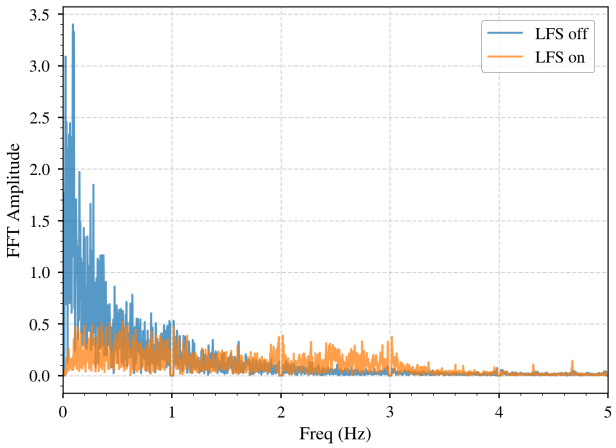

Figure 6: Normalized and filtered frequency spectrum of measured ROC during low high power operation, with and without the focal position corrector in use. As with low power operation, low frequency variations are significantly reduced by the corrector.

ACKNOWLEDGMENTS

This material is based upon work supported by the U.S. Department of Energy, Office of Science, Office of High Energy Physics, under Award Number DE-SC0021680 and Prime Contract No. DE-AC02-05CH11231.

REFERENCES

[1] E. Esarey, C. B. Schroeder, and W. P. Leemans, "Physics of laser-driven plasma-based electron accelerators", *Rev. Mod. Phys.*, vol. 81, pp. 1229–1285, 2009. doi:10.1103/RevModPhys.81.1229

[2] F. Isono *et al.*, "Update on bella center's free-electron laser driven by a laser-plasma accelerator", in *Proc. CLEO'19*, San Jose, CA, USA, 2019. doi:10.1364/CLEO_SI.2019.SF3I.1

[3] J. Einstein-Curtis *et al.*, "Laser focal position correction using fpga-based ml models", in *Proc. ICALEPCS'23*, Cape Town, South Africa, 2023, pp. 262–266. doi:10.18429/JACoW-ICALEPCS2023-TU1BCO04